International Journal of Scientific Research in Physics and Applied Sciences
Vol.11, Issue.6, pp.01-04, December 2023
E-ISSN: 2348-3423
Available online at: www.isroset.org

Research Paper

A Study of Chemically Deposited Barium Titanate ($Batio_3$) Thin Films Doped with Natural Dyes and Their Photovoltaic Applications.

C.N. Eze[1,2,3,4,5,*], A.I. Onyia[2], M.N. Nnabuchi[3]

[1,2,3,4,5]Department of Physics, Faculty of Physical Sciences, Federal University of Technology, Minna, Niger State, Nigeria. https://orcid.org/0009-0009-3900-1055.
[2,] Department of Industrial Physics, Faculty of Natural Sciences, Enugu State University of Science and Technology, Enugu, Nigeria. https://orcid.org/0000-0002-2377-8902.
[3]Department of Industrial Physics, Faculty of Natural Sciences, Enugu State University of Science and Technology, Enugu, Nigeria. https://orcid.org/0009-0003-4511-4060.
[4]Nanolab/Crystal growth laboratory, Department of Physics and Astronomy, University of Nigeria, Nsukka
[5]Lab A, Ebonyi State University, Abakaliki, Nigeria

Email address: [2]augustine.onyia@esut.edu.ng, [3]mishark nnabuchi@ESUT.edu.ng

[*]Corresponding author: marygodchrist@gmail.com, Tel: +2348038711901

Received: 29/Sept/2023; **Accepted**: 18/Nov/2023; **Published**: 31/Dec/2023. | **DOI**: https://doi.org/10.26438/ijsrpas/v11i6.14

Abstract - Ternary thin films of $BaTiO_3$ nanostructures were synthesized at 90 ^{0}C via the Chemical Bath Deposition (CBD) route under room temperature. They were doped with three natural (local/organic) dyes extracted from *Lawsonia inermis* leaves, *Beta vulgaries* roots, *and Jatropha curcas* leaves and thereafter annealed at 400 ^{0}C. doped and as-deposited nanostructures were studied employing XRD, SEM, FTIR, UV-VIS, and EDXRF. Our X-ray diffraction (XRD) studies revealed a polycrystalline structure. The SEM studies exhibited porous structures advantageous for dye loading. The EDXRF shows the compositional elements. The FTIR reveals the carboxylate and photo physical properties of the dyes. The UV-VIS investigation presented band gap energies Eg of the doped as ad (BR) = 2.60 eV; bd (OO) = 1.61 eV; ccd (LL) = 1.90 eV against the as-deposited AD (g1) = 3.10 eV showing that the dyes reduced the Eg of the thin films occurring from an increased absorption coefficient α. The Nano porous, as-deposited thin films adsorb the extracted dyes on the surface and the interaction between the Nano porous films and the natural dyes used to dope $BaTiO_3$ was studied using UV-VIS spectrophotometer with the aim of investigating their photovoltaic applications.

Keywords: $BaTiO_3$, Characterization, CBD, Doping, Organic/natural dyes, Photovoltaic applications, Synthesis.

Introduction:

The earth receives a reasonable quantity of energy from the sun measuring about 10,000 times over worldwide requirement. This abundant energy could be utilized via technological photovoltaic process that changes the energy from the sun into electrical energy. It offers a matchless and prospective solution which has gathered a very extensive consideration. There is the need to find benign processes of utilizing and proper sunlight harvesting which has led researchers to the use of sunlight-absorbing materials like the sensitizers/natural dyes which have been identified to contain pigments for light absorption and bonding. In this day and age, natural dyes are considered in educational, coloration technology, and industries because they have the characteristics of being cheap, flexible, lightweight, easy extraction and electronic tunability. It has been studied that Beetroot and many other natural dyes are lightweight and can be used as light-absorbing material in solar cells [1] . Organic dyes are presently preferred than their inorganic/commercial dyes counterparts [2],[3]. This is because they have higher absorption coefficient [4], [2], cheap, easy extraction, readily available, harmless and easily synthesized. Natural dyes have some natural pigments known as the chromophore which is the essential property of the dye that help it to absorb light and still maintain its essential color [5]. These natural dyes have been discovered to be utilized in photovoltaic devices [6], [7], [8], [9], [10], [11], [12]. Inorganic/commercial dyes like ruthenium -free dyes has been advanced with high performance but they have shortcomings such as timewasting and strenuous fabrication in addition to toxic verification before commercial utilization.

Doping involves integrating the dopant in into the lattices of the doped which results in modification of the chemical, physical and electrical properties of the doped [13] in our $BaTiO_3$. Doping with dyes usually result to an increase in the surface area of the ternary thin film. The dye molecules can easily penetrate into the ternary thin film's crystal lattice. Natural dyes are mostly used in doping because of their small size molecular radius and low material price. The concentration of the dyes has become successful in construction and more dye colorant has great effect on their important optical properties where there is broad utilization for practical solar energy harvesting, photo catalysis and photovoltaic devices. Natural dyes extracted from beetroot, henna leaves and leaves of purging nut can be used in doping the ternary metal oxides like $BaTiO_3$ which has been identified as a large area thin film [14]. Owing to their tunable characteristic, the many applications of $BaTiO_3$ semiconductor nanostructures include: photo catalysis [14], transistors [15]; catalysis [16], [17], gas sensors [18]. energy storage devices [19], energy harvesting and Optoelectronics [20]

Chemical bath deposition technique is a choice method because it encompasses a well-ordered precipitation of desired compound from the solution onto a proper substrate. It is a low cost, low temperature, reliable, simple, convenient and gives uniform deposition. CBD method when used to produce semiconductor thin films are more appropriate than the vapor phase methods. One of the commonest synthesized films via CBD is the Photovoltaic films with wide applications resulting from enhanced photovoltaic properties suggesting that films produced via CBD route offers superior photovoltaic properties than films deposited by other approaches. These photovoltaic films reveal larger size quantization, reduced crystals, enhanced optical band gap and multipurpose applications. Buffer layers in photovoltaic cells are mainly synthesized via the CBD route following the fact that substrates are not destroyed by CBD process. There are several applications of films synthesized via CBD such as. Films produced by CBD remain habitually utilized in semiconductors, photovoltaic cells and super capacitors. This has generated high curiosity in effective employment of CBD to produce nanomaterials [21], [22], [23], [24], [25].

Several techniques have been utilized by many researchers extensively to synthesize $BaTiO_3$ thin films doped with organic and inorganic dyes for various applications [26], [27], [28], [29], [14], [30], [31], [32], [33], [34] but none has synthesized $BaTiO_3$ doped with *Lawsonia inermis*, *Beta vulgaries and Jatropha curcas* via CBD route hence the motivation for this research. Though the production of $BaTiO_3$ is faraway more intricate than its binary equivalents owing to its multicomponent nature, the intricacy rises even more when targeting cheap and dye-doping procedures via chemical bath deposition methods.

Films produced by CBD and $BaTiO_3$ doped with some natural dyes have possible application in poultry protection, warming coatings, solar cell fabrication, etc. and these natural dyes have also been discovered to be utilized in photovoltaic devices.

2 Related Works

D. R. Arunkumar, et al., used CBD, screen printing (SP) and spray pyrolysis coating (SPC) techniques to synthesize Tebium (Tb) doped $BaTiO_3$ thin films. The XRD, SEM and HRTEM suggested a tetragonal phase of $BaTiO_3$ which promised a high-performance Tb doped $BaTiO_3$ photo anode of DSSC, [35]. S. Chandrappa et al., in trying to tune the carrier concentration of $BaTiO_3$ with the extension of the optical response realized a p-type $BaTiO_3$ (BTO) with visible light ($\lambda \leq 600$) absorption via iridium (Ir) doping. However, with substantial development, concurrently prompting visible light with a well-ordered carrier concentration through doping stands to be a challenge. They found out that the Ir-doped BTO has become a hopeful semiconductor that has looming utilizations in solar fuel generations and optoelectronics [36]. L. Daiming, et al., synthesized three $BaTiO_3$ nanostructures of hydrothermally deposited nanocubes, sol-gel calcined nanoparticles, and electronspun nanofibers. The nanofibers exhibited a greater piezocatalytic degradation presentation because of big specific surface area, good crystal size, and easy deformation structure as well as initial dye concentration, ionic strength and ultrasonic power. This work helps in the growth of great presentation of piezo catalysts as well as promising piezo catalysis for water remediation [37]. I. Jinchu, et al., presented results that showed the benefits of using organic dyes as against the inorganic ruthenium dyes for photovoltaic applications. They proposed using molecular engineering for the advancement of the energetic and kinetic properties of the dyes to enhance cell performance [38]. A.H. Ali, stated that top-down approach, not bottom-up methodology becomes the unsurpassed methodology which also discusses the consecutive cutting of a bulk material to get nano sized particles useful in regulating particle size, particle shape, size distribution, particle composition and degree of particle agglomeration. Semiconductor coupling, metal ion doping, nonmetallic element doping as well as sensitization/doping with organic dyes are the attributes that the improved semiconductor photo catalysts has in addition to visible light (λ = 400 nm -700 nm. He maintained that a greater photocatalytic activity of ternary nano composites can results from effective decomposition of natural dyes, and that ternary nano composites have great visible light photo catalytic activity [39]. M. Fakhar-e-Alam, et al., synthesized $BaTiO_3$ by co-precipitation technique employing barium carbonate and titanium dioxide. They applied barium titanate on breast cancer line (MCF.7) and observed a significant toxicity rate. A higher concentration inhibits breast cancer cells as their results presented and it becomes a nanomaterial for anti-cancer drug discovery [40]. R. Tas, produced $BaTiO_3$ nanoparticles quickly and at low cost via microwave technique. Obtained $BaTiO_3$, Poly aniline (PANI)/ $BaTiO_3$ nanocomposite films were sensitized and characterized. When utilized in form of a counter electrode in DSSC, the found that 39 % is the conversion efficiency proving its usage in photovoltaic applications [41].

3 Experimental Procedure

3.1 Material synthesis and dye extraction

The thin films $BaTiO_3$ were synthesized from optimized values via CBD method at room temperature. 0.3 M 1.40 g $BaCl_2.2H_2O$ was dissolved in 50 ml of water inside a 60 ml beaker. 30 ml of it were transferred into another 60 ml beaker where 5 ml of $TiCl_3$ was added and stirred using magnetic stirrer for 10 min and 5 ml of NaOH calculated at 1.0 M 0.8 g was used as a reducing agent and added into this solution and stirred for 10 min. This was allowed in a beaker for the undoped/as-deposited labelled AD(g1). For comparison between the as-deposited and different dye-doped films, separate beakers were used and labelled maintaining the same conditions. Three drops of each extracted dye from *Lawsonia inermis, Jatropha curcas* and *Beta vulgaries* were allowed per bath for the doped and labelled ccd (LL), bd (OO) and ab (BR) respectively. A glass substrate inserted into this mixture for deposition measuring 2.24 x 2.24 x 0.75 was earlier cleansed using a concentrated hydrochloric acid, detergent solutions was further used to washed it, after this, it was bathed in distilled water thereafter, allowed to desiccate in a background devoid of dust It was

inserted into this mixture through a synthetic foam for deposition in oven at 90 ^{0}C for 1 h and thereafter annealed at 400 ^{0}C for 1 h and characterized.

3.2 Characterizations

The doped and as-deposited films were examined for crystalline structure and phase properties using an advanced X-ray diffractometer (XRD) using the energetic monochromatized $C_uK\alpha l$ radiation source (λ = 1.5406 Å) which scanned films continuously as 2θ varied from 10 to 80 ^{0}C at a step size of 0.02 ^{0} and at a step time of 0.2 s. The Scanning electron microscope (SEM) was carried out using PRO:X:800-07334 Phenom World, MVE0570775 operated at 10 KV. Optical absorptions analysis regarding our products was studied using UV-VIS spectrophotometer. The presence/distribution of the elements has been investigated employing Energy Dispersive X-ray Fluoroscopy (EDXRF) using ARL QUANT'X EDXRF Analyzer, SRM 2710 at 10 min run time. The Fourier Transform Infra-Red Spectrometer (FTIR) Cary 630 was employed for investigating the chemical/electronic structure plus the existence of functional groups. We studied the transmittance of energy against wave number in a Mid-infrared spectrum (mid-IR spectrum) of the different dyes.

4.0 Results and Discussion.

4.1 X-ray diffraction study

Figure 1 depicts XRD patterns got from $BaTiO_3$ nanostructures synthesized from the precursors: $BaCl_2$ and $TiCl_3$. The figure exhibits crystalline nature of the synthesized thin films. The diffractograms have preferred orientation along the (110) plane corresponding to 2θ = 32.36 ^{0} and peaks seen were at 2Θ angles of 21.40, 32.36, 40.28, 47.25, 52.40, 58.46, 68.46, and 77.79, degrees corresponding to (hkl) orientation of 100, 110, 111, 200, 201, 211, 220 and 222 respectively. This was indexed to JCPDS 00-014-0033 $BaTiO_3$. This is close to what was got by [42]. The crystalline peaks are in phase and there is no phase segregation or extra/additional peaks noticed. The peaks of the doped, particularly LL, appeared improved with more refined, intense, high and narrow peaks than the as-deposited counterpart. This could be attributed to the dyes which has modification characteristics.

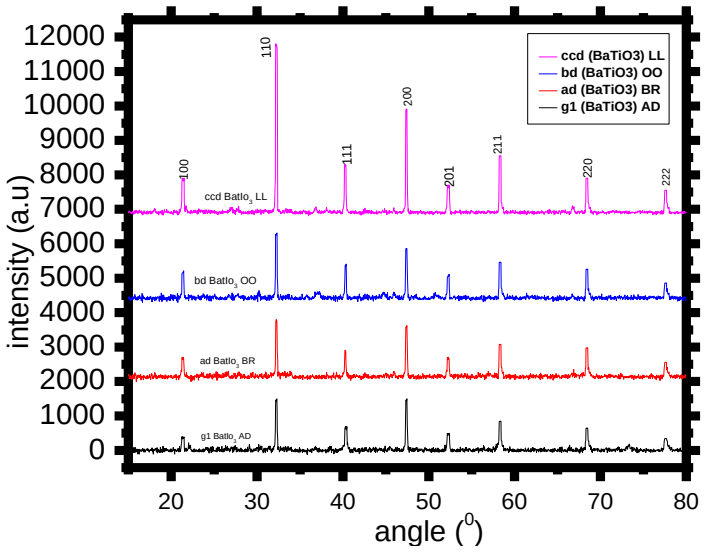

Figure 1: The XRD Pattern of CBD Deposited $BaTiO_3$ of AD and Films Doped with Different Dyes.

The crystallite grain size of $BaTiO_3$, D (nm) and other parameters shown on table 1.0 were calculated are using: Debye-Scherer's equation on (110) peak for D (nm): $D = \frac{K\lambda}{\beta Cos\theta} = \frac{0.89\,\lambda}{\beta Cos\theta}$ (1)

Lattice spacing, d (nm): $d = \frac{\lambda}{2sin\theta}$ (2)

Dislocation density, δ: $\delta = \Delta = \frac{1}{D^2}$ (3)

Lattice Strain, ε: $\varepsilon = \frac{\beta}{2sin\theta}$ (4)

where β is known as the intensity of peak's full width at half maximum (FWHM) (i.e., half the peaks width), *K* shows a constant identified as the shape factor equivalent to 0.94, λ is wavelength and has a value of (0.1542 nm) or 1.5406 Å and stands for the wavelength of the monochromatic light needed in irradiating the material. D is the crystallite size and Θ is the Bragg's angle.

The calculated parameters from equations 1, 2, 3, and 4 are shown in table 1and the values of D, d, δ and ε are seen to be 38.71784, 2.2989, 6.67E+14 and 0.286001 respectively. The fairly large crystallite size D resulted to reduced Eg and band bending effect for C-H group and O-H vibrations as seen in section 4.4, 4.5 and table 2 respectively. The inter planer distance, d, which is the vertical spacing between the parallel atomic planes in a crystal is seen to be 2.2989 and correspond to (110) planes of $BaTiO_3$. The obtained dislocation density, δ is 6.67E+14. This shows high microstrains which are commonly observed in nanocrystalline materials and is influenced by our natural dyes' molecules. This lattice strains originated from the dislocations of the unit cells

about their normal points frequently created by crystal inadequacies, non-homogeneous lattice alterations, displacements, antiphase domain boundaries. This caused peak broadening. The lattice strain, ε of 0.286001 obtained is low inferring that the interstitial impurities in the sample is highly reduced. This equally suggests reduction in disturbance in the conduction electron distribution, reduction in the distortion of the crystal lattice and reduced polarization of the electronic charge. Some properties of the obtained materials are thereby significantly changed. The addition of the dyes could be attributed to some of these occurrences. The value of ε obtained is positive which suggest that the axial strain is tensile.

Table 1: The Parameters Obtained From the XRD Data Analysis of the $BaTiO_3$

Angle (2θ)	θ in rad	FWHM (β)	FWHM (βin rad)	Crystallite Size, D (nm)	Lattice spacing, d (nm)	Dislocation density, δ	Lattice Strain, ε
16.50329	8.2516	0.48096	0.008394	32.69313	5.3671575	3.74E+13	0.82911
32.23886	16.119	0.3736	0.006521	40.856316	2.7744516	2.40E+13	0.32318
40.3402	20.17	0.4372	0.007631	34.112947	2.2339943	3.44E+13	0.29755
47.39531	23.698	0.36673	0.006401	39.671796	1.9165968	2.54E+13	0.20888
49.15368	24.577	0.43539	0.007599	33.186663	1.852069	3.63E+13	0.238
58.21445	29.107	0.21574	0.003765	64.346082	1.5835277	9.66E+12	0.09687
68.43508	34.218	0.49561	0.00865	26.509553	1.3698203	5.69E+13	0.1822
73.09328	36.547	0.3327	0.005807	38.366231	1.2935849	2.72E+13	0.11221
Average				38.71784	2.2989003	6.67E+14	0.286

4.2 morphological studies.

Figures 2, 3, 4, 5 displayed surface morphology of the films synthesized. These micrographs revealed a uniform and complete coverage of the glass slide. A large surface area is being created which is important in sunlight harvesting resulting in increased absorption by the thin films. The porosity of the films increases with the addition of dyes as suggested by the micrographs of the as-deposited and doped films. An except is BR but more in LL and this is in line with what was got by [32]. The porosity shown is advantageous in dye loading for photosensitization utilized in DSSCS. The effect is the in rise in crystalline structure of our synthesized material as shown in XRD pattern presented in figure 1. Figure 2 exhibited nanograins in ridges with few points of agglomerations. There is evidence of pin holes in figure 3 (BR) which diminished with addition of other dyes. It showed equal sized nanograins evenly/homogenously distributed. Figure 4 reveals pebble like image with increased porosity. Figure 5 shows distinct nanograins, one-sided agglomerations, presentation of white patches and higher porosity which the dye creates for dye loading, easy electron transport and better sunlight harvesting appearing more in LL. The white appearances coming from dye, noticeable in LL depicts henna dyes as a better dye than others. The dye adsorption and interaction of dye molecules with $BaTiO_3$ creates a large surface area needed for efficient sunlight harvesting. This presents the dye as organic structure with modification characteristics.

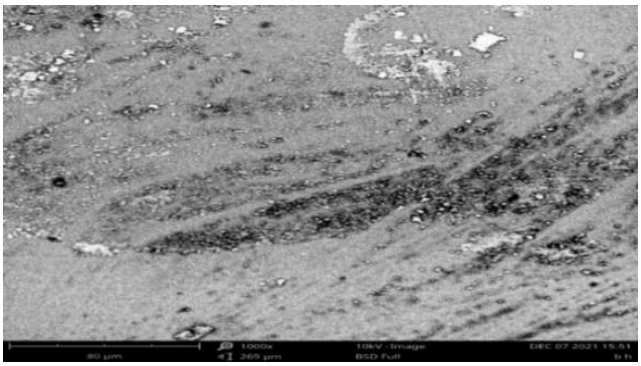

Figure 2: The SEM Micrograph of Sample g1 of $BaTiO_3$ As- Deposited (AD)

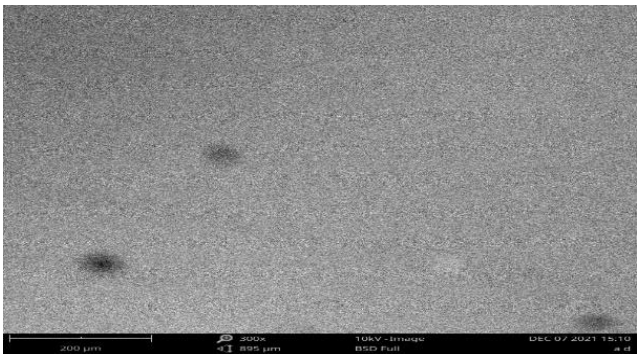

Figure 3: The SEM Micrograph of Sample ad of $BaTiO_3$ Doped with Dye3 (BR)

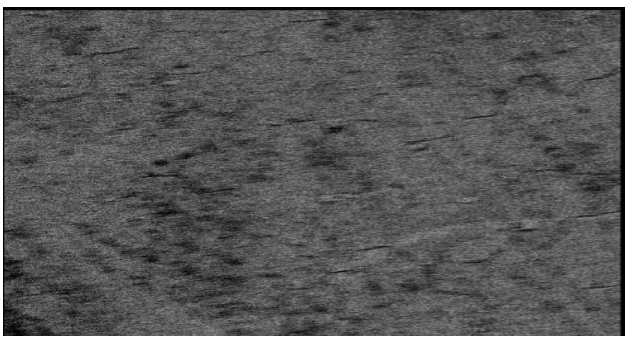

Figure 4: The SEM Micrograph of Sample bd of $BaTiO_3$ Doped with Dye2 (OO)

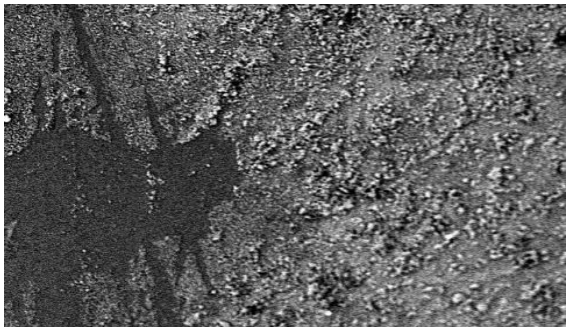

Figure 5: The SEM Micrograph of Sample ccd of $BaTiO_3$ Doped with Dye1 (LL)

4.3 Composition study.

The EDXRF results shows spectrum of sample AD (g1), ab (BR), bd (OO) and ccd (LL) of $BaTiO_3$ nanostructures establishing that the doped and as-deposited thin films have their different elements properly represented as shown in figures 6, 7, 8, and 9. Other elements found in the compound are from substrates(glass) and dyes as beetroot, henna and some other dyes is known to contain potassium, sodium, phosphorous, calcium, magnesium, copper, iron, zinc, nitrogen and manganese [43], [44], [45]. However, Barium was detected in low quantity in accordance with the earlier stated fact of its characteristic irreproducibility and strenuous deposition attributes particularly via CBD route.

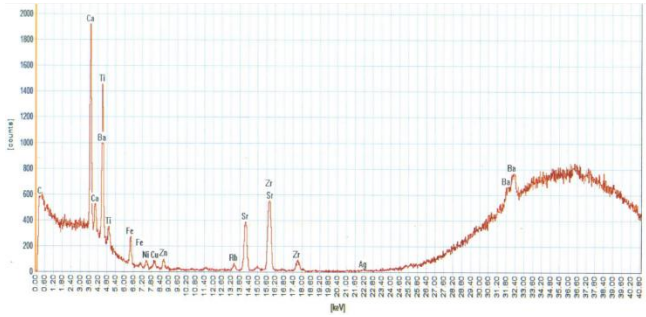

Figure 6: The EDXRF Spectrum of as-deposited Sample AD(g1)

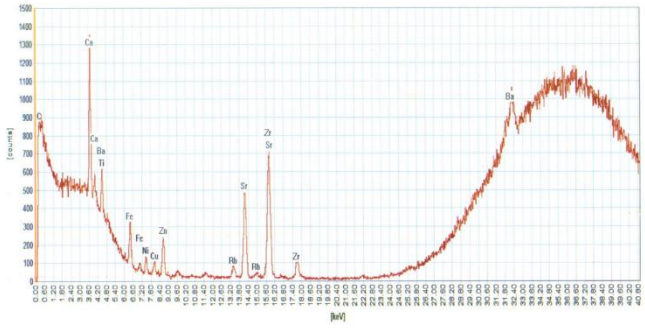

Figure 7: The EDXRF Spectrum of Sample ad Doped with Dye 3 (BR)

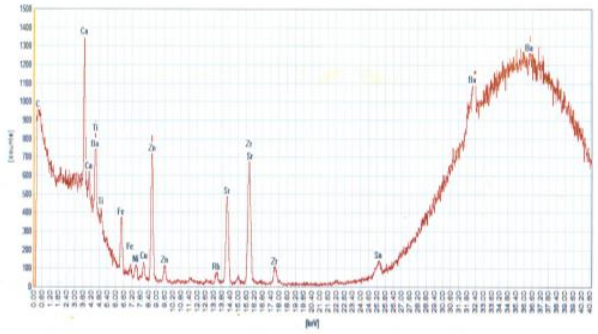

Figure 8: The EDXRF Spectrum of Sample bd Doped with Dye 2 (OO)

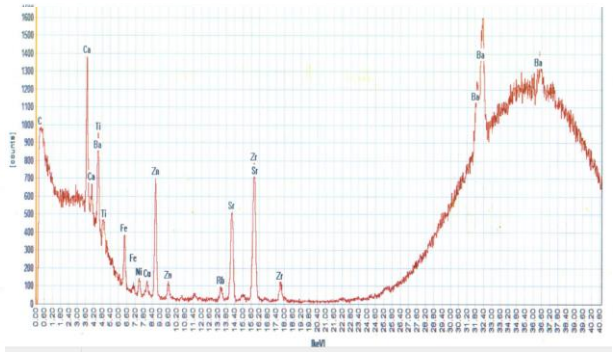

Figure 9: The EDXRF Spectrum of Sample ccd Doped with Dye 1 (LL).

4.4 Optical Studies and Band Gap Energy Analysis.

The significance differences between the doped and as-deposited are observed and some parameters got from our UV-VIS spectrophotometer highlighted most of the potential applications of this work in solar energy devices. The Optical Spectrum of as-deposited AD (g1) and doped samples (BR), (OO) and (LL) of $BaTiO_3$ are shown as presented in the spectra of absorbance, A; reflectance, R; extinction coefficient, k; transmittance, T; and energy band gap, Eg of both the undoped and dye-doped nanostructures as shown in figures 10, 11, 12, 13, and 14. These properties for the doped have dependence on the dyes used to dope the films. From figure 10, we observed, within visible region of the electromagnetic spectrum, strong absorption of the incident radiation. The samples doped with dye have higher absorbance than the as-deposited samples with LL having higher absorbance than others at wavelength range of 400 to 652.75 nm. The dye-doped samples have absorbance of 43 %, 53 %, and 71 % corresponding to BR, OO, and LL respectively within visible region of the

electromagnetic spectrum as against as-deposited AD which measures 29 %. The AD, BR, OO and LL have their corresponding absorption band edges measured as 468.5 nm, 474.3 nm, 652.7 nm and 577.8 nm respectively inferring higher absorption band edges and higher absorption coefficient for the dye doped. The AD has lower absorption band edge of 468.5 nm towards higher energy making a blue shift while the dye sensitized samples have absorption edge shifting towards lower energies (NIR) making a red shift indicating decrease in the Eg of the doped thin films.

The figure 13 shows obtained values of Eg of doped films as: ad (BR) = 2.60 eV; bd (OO) = 1.61 eV; ccd (LL) =1.90 eV and as-deposited: AD (g1) =3.08 eV determined using Tauc's equation shown in equation (5): $\alpha h\nu)^2 = A(h\nu - E_g)$ (5)

(Where, α = absorption coefficient; Eg = energy band gap; A = constant and n = ½ for direct band gap.

Energy band gap, Eg is seen to decrease with the addition of dye. This decrease will make movement of electrons faster when they jump from valence band to conduction band when photon energy absorption by valence electrons equals that of the Eg [46]. The decrease in Eg is due to fairly large crystallite size, D seen on table 1 which does not implore the shift of the absorption threshold to longer wavelength since there is no single/separable confinement of electrons and holes. This fairly large crystallite size results in reduced band bending effect and reduced Eg. Reduction in Eg is an indication that there is no presence, inside the Eg, of a great density levels having energies close to the bands which would have resulted to band tailing.

Researchers like [26] got 3.21 eV and [32] got 3.0 and 3.2 eV respectively. These are close to the experimental value and in line with our value for the AD. The researcher [34] got 3.02 eV using screen printing, 2.85 eV using CBD and 2.57 eV using spray pyrolysis methods respectively. Researcher [14] got Eg of 2.3 eV, less than experimental value but close to some values we got for the dye sensitized products. Our Eg of the dye sensitized samples shows they can be used, particularly LL, as absorber for thin film photovoltaic applications which is in line with the report of [47] who reported that films that has direct allowed Eg of about 1.9 eV or lower in addition to high absorption coefficient within visible region of the electromagnetic spectrum, was considered as hopeful absorber for thin film photovoltaic uses. Dye-doping $BaTiO_3$ films resulted to modification which could increase the absorption property and strength of the samples proving the fact that visible light absorption edge and intensity can be modulated by the dye content. Since the dyes absorb in the visible region, they can be used in DSSCs. For dyes, the absorption at visible region from 400 to 700 nm could be due to the dye molecules containing π bond. Doping BaTiO3 samples with dyes makes them have the prospective of translating majority of the incident photon energy on it. Our lowered Eg will decrease the photon energy threshold for absorption.

We ca use the knowledge gathered from this work to draw an inference on the use of our synthesized material in the absorber layer production. This would not encourage loss of incident energy. Low Eg band gap properties of the doped equally makes them good candidates for window coatings of poultry houses for keeping warmth and at the long run reduce the cost of energy consumption that can accrue from the use of kerosene in lanterns and stoves.

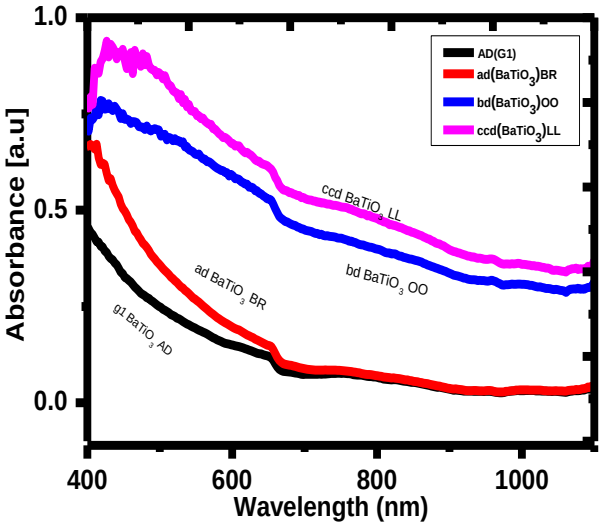

Figure 10: Absorbance Graph of $BaTiO_3$ for Doped and as-deposited Thin Films

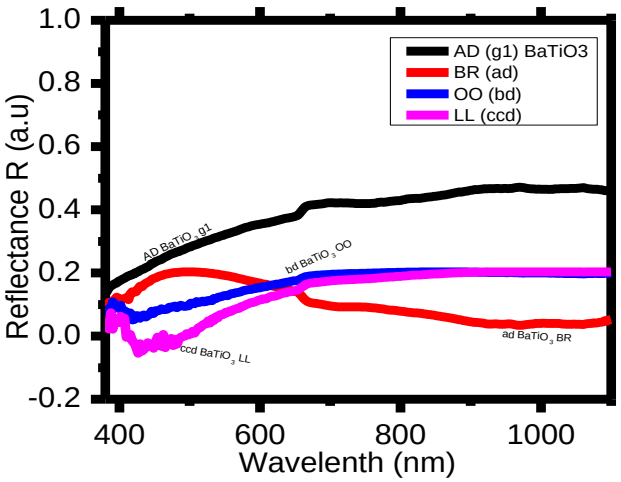

Figure 11: Reflectance Graph of $BaTiO_3$ Thin Film of AD and Films Doped with Dyes

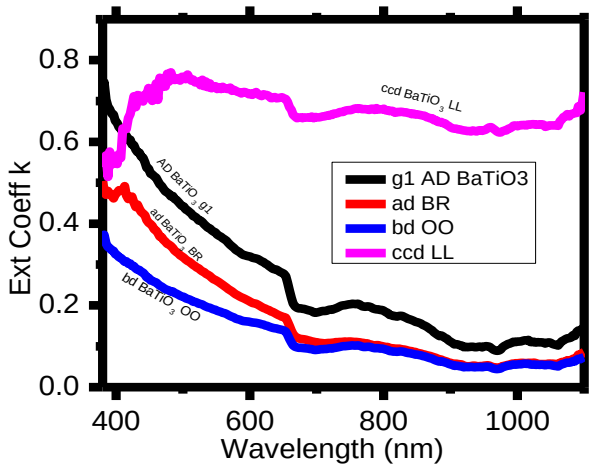

Figure 12: Extinction Coefficient Graph of $BaTiO_3$ Thin Film of AD and films Doped with dyes

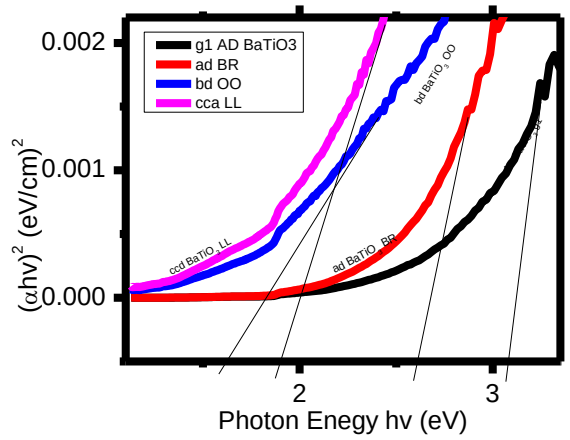

AD (g1) = 3.10 eV; ad (BR) = 2.60 eV;
bd (OO) = 1.61 eV; ccd (LL) = 1.90 eV
Figure 13: Energy Band Gap Graph of $BaTiO_3$ Thin Film of AD and Films Doped with Dyes

The figure 11 shows the as-deposited sample, AD, having higher reflectance than doped ones. All the samples show increase in reflectance as the wavelength increases from 400 nm to 650 nm in the visible region and then gradual increase up to 800 nm except sample BR which showed strong increase up to 500 nm and then started a decrease in reflectance from 500 nm to 800 nm as the wavelength increased. A lowered reflectance as seen in figure 11 and the higher absorbance emanating from higher absorption band edges and absorption coefficient of the dye-doped nanostructures compared to the AD films informs a decreasing energy in the visible region. This caused a red-shift and made BaTiO3 to be identified as high absorbance material which can be used in construction for the roofs in temperate regions where all the UV lights are absorbed and more heat is reradiated and the temperature goes up. It is positive essential contemplation utilizable in construction industry because a structure where a roof sits will not experience cooling if it has a small quantity of solar reflectance which will result in absorbing a great deal of solar heat energy. The AD samples, comparatively has higher reflectance and when applied in construction industry will reflect the UV light thereby cooling the structure and eventually reducing Air Conditioner (AC) usages. On the other hand, from the spectrum, the average optical reflectance of all samples is very low of about (0.1) 10 %. This can give high efficiency if used in the construction of solar panels because it reduces the amount of solar energy that would have reflected.

The figure 12 shows extinction coefficient k of $BaTiO_3$ samples for both AD and doped samples which shows decrease in doping with increase in wavelength as absorption coefficient increases with dye addition due to decrease in Eg and fairly large crystallite size. The variation of the extinction coefficient k of the sample was calculated using:

$$k = \frac{\alpha\lambda}{4\pi} \qquad (6)$$

For AD-g1, k decreased from 0.69 to 0.44 by varying the wavelength from 380 to 493.60 nm; for BR-ab, k reduces from 0.49 to 0.33 by varying the wavelength from 380 to 480.16 nm, for OO-ba, k drops from 0.35 to 0.20 by varying the wavelength from 380 to 507.04 nm and for LL-cca/ccd, k drops from 0.75 to 0.69 when raising

the wavelength from 480 to 656.16 nm. It is clearly seen that there is strong k from 380 to each maximum wavelength and weak k up to 700 nm wavelength. This signifies that the incident light is rapidly absorbed in 380 to each maximum wavelength, gradually decreases up to 700 nm and above 700 nm indicating that damping is minimal.

The lowered extinction coefficient of the doped samples shows that the product could be utilized as window layer in solar cell applications.

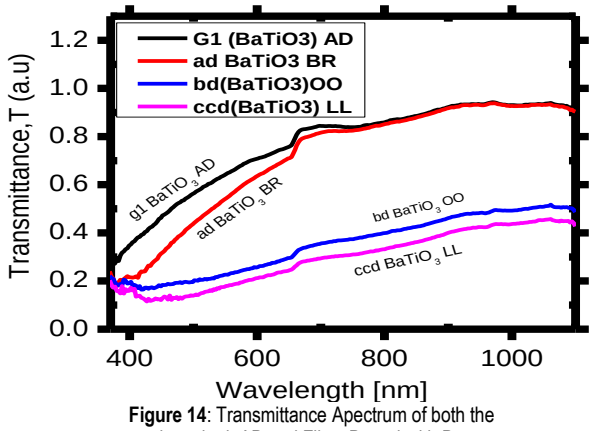

Figure 14: Transmittance Apectrum of both the as-deposited, AD and Films Doped with Dyes.

Figure 14 shows the transmittance spectrum of both the as-deposited, AD and the samples doped with dyes. The AD and BR samples have higher transmittance than the other doped samples. There is indication of lowered transmittance of the doped materials. The transmittance spectrum shows that the transmittance increases with wavelength but varies with dyes. The samples LL and OO maintain great transmittance which is about 50 % within near infrared region (NIR). Samples like AD and BR maintain great transmittance which is beyond 60 % within near infrared region (NIR) close to the transmittance value of above 50 % reported by [48]. The characteristics of great transmittance within near infrared region (NIR) which the thin films revealed presents them as useful products used for building of poultry roofs and walls and window coatings. The idea reported by [48] informs that high amount of infrared radiation will be transmitted in a poultry house to maximally eradicate cold for the chicks thereby saving cost associated with kerosene in a lantern and stoves and bills for bulbs.

Figures 15, 16, and 17 depict the schematic mid infra-red (mid-IR) spectrum of as-deposited, AD and doped BR, OO and LL samples of $BaTiO_3$ within the range of 500 to 4000 cm^{-1} of the solar radiation. In order to ascertain the presence of the functional groups and chemical structures together with bending and stretching properties, we studied the transmittance of energy against wave number of the different dyes using FTIR. This is a characterization method that reports a set of absorption frequency/transmittance in addition to peaks displayed by its wave number which portrays functional groups and kinds of bonds existing in a biological compound [49]. Broad absorption band exists in the three dyes relating the presence of hydrogen bonding. All belong to the functional group of hydroxyl group. D1 has stretching vibrations; D2 has bending and stretching while D3 has stretching. D1 and D3 have several absorption bands in the entire IR spectrum indicating both are complex structures. D2 has few absorption bands hence simple molecule/structure. Finger print region is observed in all the dyes. Table 2 shows the strong absorption spectrum within 3550—3200, 2854—2926, 2855—2975, 1432—1621, 1150—911 and 858—733 cm^{-1} which indicates bending in hydroxyl compound/O—H vibrations; stretching in Methyl group; Bending in Cyclo alkane; Stretching in Aromatic ring group; Stretching in C—O—C group and Bending in C—H group apportioned according to the obtained wave number and corresponding transmittance values depicted in figures 16, 17, and 18 for different dyes.

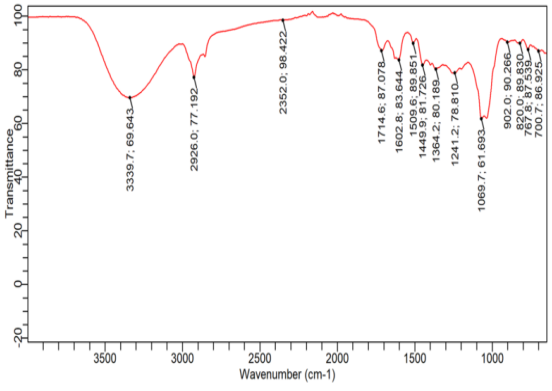

Figure 15: Mid-IR Transmittance Spectrum Regions of Henna (Laali) Dye1 (LL)

4.5 FTIR Studies

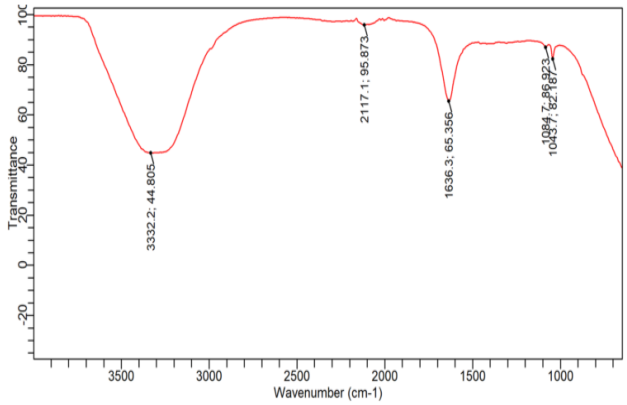

Figure 16: Mid-IR Transmittance Spectrum Regions of Purging nut Dye 2 (OO).

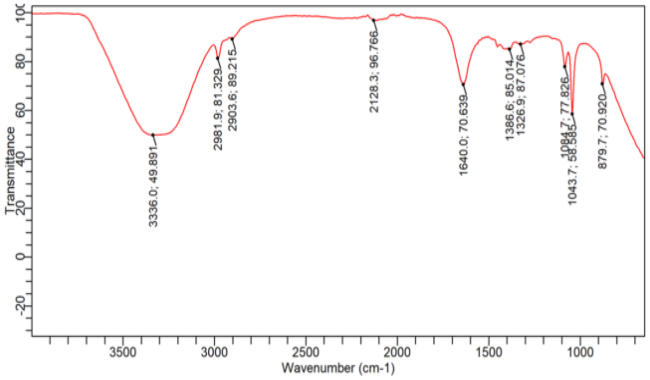

Figure 17: Mid-IR Transmittance Spectrum Regions of Beetroot Dye3 (BR)

The detailed study of the FTIR showing different functional groups is depicted in table 2. The bending and stretching vibrations specific to their different and corresponding wavelengths resulted from fairly large crystallite size that led to reduced Eg rooted in dye addition. The dyes' characteristics of bending, stretching and tailing offers stability, fast/flexibility and broadening of photoluminescence peak respectively in the synthesized samples.

Table 2. FTIR investigation showing functional groups and vibrations existent.

Wavenumber Range (Cm^{-1})	Kinds of vibrations	Functional groups
3550—3200	Bending	O—H vibrations
2854—2926	Stretching	Methyl group
2855—2975	Bending	Cyclo alkane
1432—1621	Stretching	Aromatic ring group
1150—911	Stretching	C—O—C group
858—733	Bending	C—H group
550—690	Bending	C—Cl group

Conclusion and Future Scope

The synthesis, via CBD technique, of as-deposited plus sensitized ternary nanostructures of $BaTiO_3$ on substrate slides followed by annealing reveals polycrystallization of the films without much significant effect on the dye-doped structural pattern. The thin films of the $BaTiO_3$ maintains a preferred orientation in the (110) plane as established by the XRD pattern. The surface studies revealed that the dyes had essential influence occurring at the surface configuration of the synthesized products outlining porous structures which is advantageous for dye loading utilizable in DSSCs. It created a large surface area for sunlight harvesting. The analysis of the optical studies involving Eg inferred that the Eg of the doped materials were significantly reduced resulting from the high absorption coefficient α, inferring that the materials possibly will have utilization in solar absorber layer in the manufacture of photovoltaic cell. The great transmittance in the near infrared (NIR) and low Eg revealed according to the products consequently brands them decent products for the building of roofs and walls and window coatings of poultry structures. Due to the low reflectance of the materials, it could give high efficiency if used in solar panels because it reduces the amount of solar energy that would have reflected. This proves an actual significant contemplation for the building engineering. The lowered extinction coefficient of the doped samples shows that the materials can be used in window layer in solar cell applications.

Data Obtainability

The researchers approve that the records backing up the results of this research remain obtainable from the corresponding author [C.N. Eze] on rational demand.

It was a very ugly experience carrying out this research without any financial support from anywhere. Authors therefore resorted to using simple techniques.

Conflict of Interest

None

Funding Source

None

Authors Contribution

Calister Ngozi EZE carried out most of the experimental work and data analysis. Mishark N. NNABUCHI was involved in the experimental design and Augustine I. ONYIA was involved in the manuscript editing and proof reading of the manuscript.

Acknowledgements

I want to express gratitude to my respected guide, Dr. V. Chukwuma, Professor of Physics, Physics Department, Akwa Ibom State University, Nigeria and Dr A. I. Chima, Physics Department, Enugu State University of Science and Technology, Enugu, Nigeria for giving their scholarly motivation and proper guidance.

AUTHORS PROFILE

Calister Ngozi EZE is currently doing her Ph.D. (Physics) degree in solid state physics/material science from Enugu State University of Science and Technology, Enugu, Nigeria. Her main study area is on synthesis of nano materials. She obtained her Bachelor of Science from Enugu State University of Science and Technology, Enugu, Nigeria. She obtained her Post-Graduate Diploma in Computer [PGDC] from Abubakar Tafawa Balewa University Bauchi, Nigeria. She obtained her Postgraduate Diploma in Management [PGDM] from Abubakar Tafawa Balewa University Bauchi, Nigeria. She obtained her Master of Business Administration [MBA (General)] from Abubakar Tafawa Balewa University Bauchi, Nigeria. She obtained her M.Sc. Physics (Bio Physics) from University of Jos, Plateau State, Nigeria. Her research interests are Biophysics/medical physics, Thin film Fabrication and Characterization, Nanotechnology Sciences and Solar Energy Technology. She has several publications in sound, peer reviewed, international Journals/Conferences, majority of which are online. She is currently working in Department of Physics, Federal University of Technology, Minna, Niger State, Nigeria. She has many years of teaching experience and research involvement. She is a member of two professional bodies: Member, Nigerian Institute of Physics, (MNIP) and Member, Nigerian Institute of Management (MNIM).

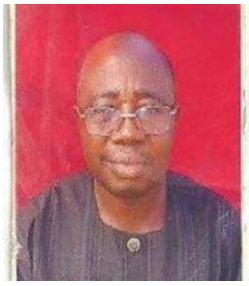

Augustine Ike ONYIA has B.Sc. Physics and M.Sc. Solid State Physics in the University of Nigeria, Nsukka, Nigeria and Ph.D. in Ebonyi State University, Abakaliki, Nigeria. He works in the Department of Industrial Physics, Enugu State University of Science and Technology, Enugu, Nigeria. His research interests are: Thin Film Fabrications, Nanotechnology, Material Sciences and Solar Energy Technology. He has published many research papers in reputed, peer-reviewed and citations indexed in local and international journals/conferences. He is a Professor of Solid-State Physics.

Mishark Nnamdi NNABUCHI holds Bachelor of Science Degree, Master of Science Degree and Doctor of Philosophy of Science Degrees in Physics and Astronomy of the University of Nigeria, Nsukka. Currently, M.N. Nnabuchi is the Head of the Department of Industrial Physics, Enugu State University of Science and Technology, Enugu. His area of specialization is Solar Energy Physics/Material Science. His research interests are Thin film Fabrication and Characterization, Nanotechnology Sciences and Solar Energy Technology. He has published over 90 research papers in a reputable peer-reviewed and citation-indexed journals. His is a member of so many professional bodies, like NIP, SESN, MSN etc. He has successfully supervised about 10 Ph.D. students and 20 Masters students. He is a Professor of Physics and Astronomy.

REFERENCES

[1] N. S. Kumari, "Polyvinyl alcohol/beetroot dye film as light absorbing material in solar cell.," in *AIP Conf. Proc.* , AIP Publishing, Alappuzha, Kerala,, 2020.

[2] G. Emre, D. B. S. A. Veysel, C. Mert, F. T. Omer, S. Tugba, I. Mehmet, N. Mehmet and S. Ilkay, "Photovoltaic performance and photostability of anthocyanins, isoquinoline alkaloids and betalains as natural sensitizers for DSSCs.," *Solar Energy,* vol. 173, p. 34—41., 2018.

[3] K. V. Bharath, B. Shoumitra, T. Ramachandran and K. S. Rajni, "Extraction and absorption study of natural plant dyes for DSSC.," *International Journal of ChemTech Research,* vol. 9, no. 1, p. 254—258, 2016.

[4] C. C. Y. H. Yung-Chung, Y. L. Ryan and H. Kuo-Chuan, "Materials for the active layer of organic photovoltaics: Ternary solar cell approach.," *ChemSusChem,* vol. 6, p. 20—35, 2013.

[5] F. A. R. J. Paredes-Lopez and O. Delgado-Vargas, "Natural pigments: Carotenoids, anthocyanins andbetalains – Characteristics, biosynthesis, processing and stability.," *Critical Reviews in Food and Science and Nutrition,* vol. 40, no. 3, p. 73—289, 2000.

[6] P. N. Paudel, A. Pandey, R. R. Shrestha, A. Neupane, P. Lamichhane, R. Adhikari, R. Gyawali and K. B. P., "Optical properties of natural dyes: prospect of application in dye sensitized solar cells (DSSCs) and organic light emitting diodes (OLEDs)," *Food Research,* vol. 2, no. 5, p. 429—436., 2018.

[7] W. A. Dhafina and D. H. M. Salleh, "The sensitization effect of anthocyanin and chlorophyll dyes on optical and photovoltaic properties of zinc oxide based dye sensitized solar cells," *Optik.,* 2019.

[8] O. S. Y. Awodugba and A. O. Adedokun, "Solvent dependent natural dye extraction and its sensitization effect for dye sensitized solar cells," *Optik,* vol. 6, p. 64., 2018.

[9] C. G. D. M. Giuseppe, C. Stefano, C. Silvia, A. Oberto and A. B. Caralo, "Natural dye sensitizers for photoelectrochemical cells.," *Energy & Environmental Science,* vol. 2, p. 1162—1172, 2009.

[10] H. T. N. Satoshi, O. Hideo, B. Hiroaki and I. Shinzaburo, "Hide Improvement of the light-harvesting efficiency in polymer/fullerene bulk heterojunction solar cells by interfacial dye modification.," *Applied Materials & Interfaces,* vol. 1, no. 4, p. 804—810., 2009.

[11] H. Satoshi, B. Hiroaki and I. Shinzaburo, "Multi-coloured dye sensitization of polymer/fullerene bulk heterojuction solar cells," *Chem.Commun.,* vol. 46, p. 6696—6598., 2010.

[12] Z. M. N. S. Shuhua, L. Feng, Z. Zhongqiang, H. Qin, P. R. Thomas, S. Minmin, L. Chang-Zhi and C. Hongzheng, "Effecient and 1,8-diiodooctane-free ternary organic solar cells fabricated via nanoscale morphology tuning using small-molecule dye additive.," *Nano Research,* vol. 27, no. 5, pp. 34-39, 2017.

[13] K. S. Rao and T. Vanaja, "Influence of transition metal (Cu, Al) ions doping on structural and optical properties of ZNO nanopowders.," in *4th International Conference on Materials Processing and Characterization*, Haryana, 2015.

[14] D. Masekela, N. C. Hintshow-Mbita, S. Sam, T. N. Yusuf and N. Mabuba, "Application of BaTiO3 -based catalysts for piezocatalytic, photocatalyric and piezo-photocatalytic degradation of organic pollutants and bacterial disinfection in waste water: A comprehensive review.," *Arabian Journal of Chemistry,* vol. 16, no. 2, pp. 1044-73, 2023.

[15] O. F. Shoron, S. Raghavan, C. R. Freeze and S. Stemmer, "BaTiO3/SrTiO3. Heterostructures for ferroelectric field effect transistors," *Appl. Phys. Lett.,* vol. 110, p. 232902, 2017.

[16] C. Srilakshmi, G. M. Rao and R. Saraf, "Effect of the nature of a transition metal dopant in the BaTiO3 perovskites on the catalytic reduction of nitrobenzene," *RSC ADV.,* vol. 14, no. 2, pp. 6789-6793, 2015.

[17] Q. Tang, J. Wu, D. Kim, C. Franco, A. Terzopoulou, A. Veciana, J. Puigmarti-Luis, X. Chen, B. J. Nelson and S. Pane, "Enhanced piezocatalytic performance of

BaTiO3 nanosheets with highly exposed (001) facets," *Adv. Funct. Mater.,* vol. 32, p. 2202180, 2020.

[18] S. Park and D. Seo, "Gas sensing characteristics of BaTiO3-ceramics," *Mater. Chem. Phys.,* vol. 85, pp. 47-51, 2004.

[19] N. Acout, H. S. Refai, M. A. Kebede, F. Salman and E. Sheha, "Significant study of BaTiO3 as a cathode for mangnesium battery applications.," *Mater. Chem. Phys.,* vol. 292, p. 126770, 2020.

[20] A. Karvounis, F. Timpu, V. V. Vogler-Neuling, R. Savo and R. Grange, "BaTiO3: Barium titanate nanostructures and thin films for photonics," *Adv. Opt. Mater.,* vol. 8, p. 2070094, 2020.

[21] P. K. Nair, M. T. S. Nair, V. M. Garcia, O. L. Arenas, A. Pena, Y. Castilo, O. Gomezdaza, A. Sanchez, J. Campos, H. Hu and R. Suarez, "Semiconductor thin films by chemical bath deposition for solar energy related applications," *Solar Energy Materials and Solar Cells,* vol. 52, no. 3, pp. 313-344, 1998.

[22] M. K. D. Guire, L. P. Bauermann, H. Parikh and J. Bill, "Chemical bath deposition", Chemical solution deposition of functional oxide thin films.," *Springer,* pp. 319-339, 2021.

[23] G. Hodes, "Semiconductor and ceramic nanoparticle films deposited by chemical bath deposition," *Physical Chemistry Chemical Physics,* vol. 9, no. 18, pp. 2181-2196, 2007.

[24] S. Tec-Yam, R. Patino and A. I. Oliva, "Chemical bath deposition of CdS films on different substrate orientations," *Current Applied Physics,* vol. 11, no. 3, pp. 914-920, 2011.

[25] M. T. S. Nair and P. K. Nair, "Simplified chemical deposition technique for good quality SnS thin films," *Semiconductor Science and Technology,* vol. 6, p. 132, 1991.

[26] M. G. Elmahgary, A. M. Mahran, M. Ganoub and S. O. Abdellattif, "Optical investigation and computational modelling of BaTiO3 for optoelectronic devices applications.," *Springer Nature,* vol. 7, no. 2, pp. 345-350, 2023.

[27] M. D. Gomes, L. G. Magalhaes, A. R. Paschoal, Z. S. Macedo, A. S. Lima, K. I. B. Eguiluz and G. R. Salazar-Banda, "An eco-friendly method of BaTiO3 nanoparticles synthesis using coconut water," *Journal of Nanomaterials,* vol. 7, p. 182, 2018.

[28] A. S. Ameer and A. Aadil, "Degradation of organic and toxic pollutants by embedding the barium titanate nanoparticles in polyaniline matrix (BaTiO3@PANI).," in *IOP Conf.Series: Material Science and Engineering*, 2019.

[29] K. I. Osman, "Synthesis and characterization of BaTiO3 ferroelectric material.," Cairo Uni.,, Giza, 2011.

[30] P. Aktas, "Synthesis and characterization of BaTiO3 nanopowder by pechini process," *Cetal Bayar University Journal of Science,* vol. 16, no. 3, pp. 293-300., 2020.

[31] D. Liu, C. Jin, F. Shan, J. He and F. Wang, "Synthesizing BaTiO3 nanostructures to explore morphological influence, kinetics and mechanism of piezocatalytic dye degradation," *Applied Materials and Interfaces,* vol. 12, pp. 17443-17451, 2020.

[32] K. G. Baiju, B. Murali and D. Kumaresan, "Synthesis of hierarchical barium titanate micro flowers with superior light harvesting characteristics for dye sensitized solar cells," *Material Research Express,* vol. 10, no. 2, pp. 4322-4329, 2018.

[33] K. C. Huang, T. C. Huang and W. F. Hsieh, "Mophology controlled synthesis of BaTiO3 nanostructures.," *Inorg. Chem,* vol. 48, pp. 9180-9184., 2009.

[34] D. R. Arkunkumar, S. A. U. Portia and K. Ramamoothy, "Design and fabrication of novel Tb doped BaTiO3 thin film with superior light-harvesting characteristics for

dye sensitized solar cells," *Surfaces and interfaces,* vol. 20, pp. 30845-30852, 2020.

[35] D. R. Arunkumar, S. A. U. Portia and K. Ramamoorthy, "Design and fabrication of novel Tb doped BaTiO3 thin film with superior light-harvesting characteristics for dye sensitized solar cells.," *Surfaces and Interfaces,* vol. 20, pp. 30845-30852, 2020.

[36] S. Chandrappa, S. J. Galbao, P. S. S. R. Krishnan, N. A. Koshi, S. Das, S. N. Myakala, S. C. Lee, A. Dutta, A. Cherevan, S. Bhattacharjee and D. H. K. Murthy, "Iridium-doping as a strategy to realise visible-ligth absorption and p-type behaviour in BaTiO3.," *J. Phys. Chem. C,* vol. 127, pp. 12383-12393, 2023.

[37] L. Daiming, J. Chengchao, S. Fukai, H. Junjing and W. Fei, "Synthesizing BaTiO3 nanostructures to explore morphological influence, kinetics, and mechanism of piezocatalytic dye degradation.," *Appl. Mater. Interfaces,* vol. 12, pp. 17443-17451, 2020.

[38] I. Jinchu, C. O. Sreekala and K. S. Sreelatha, "Dye sensitized solar cell using natural dyes as chromophores - Review.," *Materials Science Forum,* vol. 771, pp. 39-51, 2014.

[39] A. H. Ali, "Review on the synthesis method of nano composites and approach to making semiconductors visible ligth active.," *Curr. Synthetic Sys. Biol.,* vol. 10, no. 6, p. 1000015, 2022.

[40] M. Fakhar-e-Alam, S. Samira, H. Nazia, S. Aamir, . Inaam, S. Amjad, . Muhammad and S. Malik, "Synthesis, characterization, and application of BaTiO3 nanoparticles for anti-cancer activity," *Journal of Cluster Science,* vol. 34, pp. 1745-1755, 2023.

[41] R. Tas and M. Gulen, "Synthesis of BaTiO3 via microwave method and application of PANI/BaTiO3 nanocomposite as counter electrod in high performance dye sensitised solar cell.," *Int. J. of Inovative Engineering and Applicaications,* vol. 5, no. 2, pp. 2587-1941, 2021.

[42] K. Tewatia, A. Shama, M. Shama and A. Kumar, "Factors affecting morphological and electrical properties of Bariun titanate: a brief review.," *Materials Today: proceedings,* vol. 10, no. 513, pp. 2214-7853, 2020.

[43] B. Hathan and B. S. Singh, "Chemical composition, functional properties and processing of beetroot—a review," *Int. J. Sci. Eng. Res.,* vol. 5, no. 1, p. 679–84., 2014.

[44] P. Sakuntala, R. S. Raju and K. A. Jaleeli, "FTIR and energy dispersive X-ray analysis of medicinal plants, Ocimum gratissimum and ocimum tenuiflorum.," *International Journal of Scientific Research in Physics and Applied Research.,* vol. 7, no. 3, pp. 6-10, 2019.

[45] A. Boubaya, N. Marzougui, L. B. Yahia and A. Ferchichi, "Chemical diversity analysis of Tunisian Lawsonia inermis L. populations," *African Journal of Biotechnology,* vol. 10, no. 25, pp. 4980-4987, 2011.

[46] A. A. Elbadawi, S. I. Hamza, A. S. Hamed and Y. A. Alsabah, "Synthesis and Solar Cell Application of Dye Sensitized Magnesium Oxide MgO.," *International Journal of Scientific Research in Physics and Applied Sciences,* vol. 10, no. 3, pp. 49-54, 2022.

[47] T. Watanabe and M. Matsui, "Improved Efficiency of CuInS2-Based Solar Cells without Potassium Cyanide Process.," *J. Appl. Phys.,* vol. 38, no. 12A, p. 1379, 1999.

[48] S. C. Ezugwu, F. I. Ezema and P. U. Asogwa, "Synthesis and characterization of ternary CuSbS2 thin films: Effect of deposition time," *Chalcogenide Letters,* vol. 7, no. 5, p. 341—348., 2010.

[49] M. Jacox, "Vibrations of polyatomic transient molecules," *Journal of Physical and Chemical Reference Data,* vol. 32, p. 1 ., 2003.

